NUMERICAL AND EXPERIMENTAL ANALYSIS OF THE INFLUENCE OF THERMAL RESIDUAL STRESSES ON MATRIX FAILURE

E. Correa*, V. Mantič, F. París

Group of Elasticity and Strength of Materials, Continuum Mechanics Dpt., School of Engineering, University of Seville, Camino de los Descubrimientos s/n, 41092 Sevilla, SPAIN
**ecorrea@us.es*

Keywords: Thermal stresses, Curing, Modelling, Matrix failure, Micromechanics

Abstract
The influence at micromechanical scale of thermal residual stresses, originating in the cooling down of the curing process of fibrous composites, on matrix failure under transverse tension is studied. The effect of these stresses on the appearance of the first debonds is discussed analytically, while later steps of the damage mechanism are analysed using of single fibre models by BEM. The results are evaluated by means of Interfacial Fracture Mechanics. The conclusions obtained show that thermal residual stresses have a protective effect against failure appearance and initiation, whereas the morphology of the damage is not significantly affected. Experimental tests are carried out, the results agreeing with the conclusions derived from the numerical analysis.

1 Introduction
If knowledge of the mechanisms of failure at micromechanical level is considered to be fundamental for the development of failure criteria able to perform a more complete diagnosis of the appearance of these mechanisms [1], the analysis of the influence of curing stresses at this scale then becomes highly relevant.

The particular case of inter-fibre (matrix) failure under transverse tension has already been the object of several micromechanical studies by the authors, [2, 3], for single fibre case or dilute packing. These studies have made it possible to understand the initiation of failure at the micromechanical scale as well as its later progress, which leads to the macro-failure of the material, without considering the presence of thermal residual stresses. The results obtained assumed that crack nucleation is controlled by the radial stress generated between fibre and matrix and showed that the maximum values are placed at the angles 0º and 180º with respect to the tension applied, Fig. 1a.

Once a small debonding crack is supposed to appear (in particular, one of 10º length centred at 0º was assumed) single-fibre BEM models were employed for the characterisation of crack growth. The results produced by the BEM model, for the case in which the thermal residual

stresses are not considered, were analysed following the energetic approach of Interfacial Fracture Mechanics. Based on [4] they predicted an unstable growth of the interface crack up to a position characterized by a debonding angle $\theta_d = 60º–70º$, Fig. 1b. The study also showed that the end of unstable growth coincides with the development of a physically relevant contact zone at the crack tip.

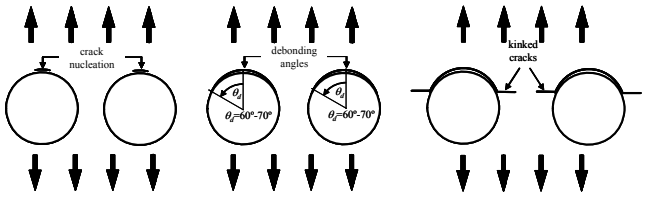

Figure 1. Micromechanical phases of inter-fibre failure under unidirectional tension.

For the case in which the thermal residual stresses are not considered, the third step of the analysis, Fig. 1c, ascertained the condition under which the interface crack would find it easier to kink into the matrix than to continue growing along the interface. The coalescence of these kinked cracks caused the appearance of a macromechanical failure which, as expected and confirmed from the experiments [3], was oriented perpendicularly to the external load.

The present work is a continuation of the previous studies of the authors related to inter-fibre failure under transverse tension [2, 3]. The objective now is to analyse the influence of thermal residual stresses originated by the cooling down associated to the curing process on the conclusions obtained so far about the different micromechanical phases of the mechanism of damage. Experimental tests are also carried out.

Material	Matrix (epoxy)	Fibre (glass)
Poisson coefficient, ν	0.33	0.22
Young modulus, E (MPa)	$2.79\text{x}10^3$	$7.08\text{x}10^4$
Thermal expansion coefficient, α ($ºC^{-1}$)	$52\text{x}10^{-6}$	$7\text{x}10^{-6}$

Table 1. Thermoelastic properties of the materials.

2 Numerical analysis

2.1 Model

The study has been carried out using a computational tool based on Boundary Element Method. The basic model employed, Fig. 2a, represents a crack that, under plain strain, grows along the interface. The second model, Fig. 2b, is employed when the kinking of the interface crack is considered.

The Energy Release Rate, G, will be used in the form of an expression based on the Virtual Closure Crack Technique, for a circular crack that propagates from a certain debonding angle, θ_d, Fig. 1a, to $\theta_d + \Delta\theta_d$:

$$G(\theta_d,\Delta\theta_d)=\frac{1}{2\Delta\theta_d}\int_0^{\Delta\theta_d}\{\sigma_{rr}(\theta_d+\theta)\Delta u_r(\theta_d-\Delta\theta_d+\theta)+\sigma_{r\theta}(\theta_d+\theta)\Delta u_\theta(\theta_d-\Delta\theta_d+\theta)\}d\theta \quad (1)$$

where σ_{rr} and $\sigma_{r\theta}$ represent, respectively, radial and shear stresses along the interface, and Δu_r and Δu_θ the relative displacements of the crack faces. When kinking towards the matrix is considered an expression analogous to (1) and corresponding to a straight crack in a homogeneous material is used.

Properties of the materials used in the numerical analysis are included in Table 1. The fibre radius considered has been $a = 7.5 \cdot 10^{-6} m$. Dimensionless results for G will be presented in all cases, in a similar way as in [3].

Finally, it is considered that the contraction of the matrix dominates the generation of thermal residual stresses during the cooling down. This fact allows the inclusion of these stresses in the analysis by means of an adequate thermal decrease (80ºC in the present case) that captures the real curing contraction (0.4%) of the material.

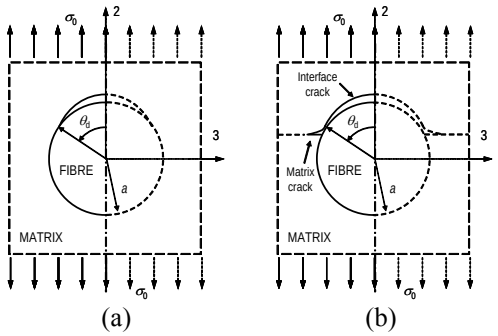

Figure. 2. Single fibre models: a) with interface crack only, and b) with interface kinked crack.

2.2 Origin of damage

The beginning of the inter-fibre failure under transverse tension is considered to be controlled by the radial stress that acts at the fibre-matrix interface, under the hypothesis of an initially undamaged material. If the external tension is the only load considered, it can be verified [3] that the zones of maximum radial stress, and therefore susceptible of housing the first debonds, are located at $\theta = 0º$ and $180º$. Thus, the analysis of the effect of thermal residual stresses on the initiation of failure must be carried out under the same premise, studying the distribution of stresses around the interface when the fibre-matrix system suffers a thermal decrease corresponding to the curing contraction of the matrix. The consideration of real curing parameters, as detailed in Section 2.1, unavoidably leads to the choice of σ_0 corresponding to failure values. In particular, the transverse tensile strength of the unidirectional laminate chosen for the bimaterial system considered has been $Y_T = 35\text{MPa}$.

In this situation, an analysis of the stress state in a single fibre-configuration, assuming the interface to be initially in perfect condition and considering a temperature decrease of 80ºC as a single external load, would allow the order of the thermal residual stresses to be estimated and their effect on the initiation of damage predicted.

The problem presented in these terms can be solved analytically (plane strain problem of a fibre embedded in an infinite matrix) and the solution obtained shows that residual stresses are only produced in the radial direction, σ_{rr}, and angular direction, $\sigma_{\theta\theta}$. These stresses are proportional to the thermal decrease and only depend on the radial coordinate. Besides, σ_{rr} presents a compressive character and maintains a constant value along the whole interface, for the bi-material system under consideration being $\sigma_{rr} = -10M\text{Pa}$.

The thermal residual compressive radial stresses detected at the interface would inhibit the appearance of the inter-fibre failure, since they involve an apparent additional strength having to be surmounted by the stress state to produce the first debonds, though their location would not be altered. In any case, comparing the residual stress level (-10 MPa) with the transverse tensile strength (35 MPa) it can be deduced that, though of the same order, the stress due to the external load is dominant.

2.3 Interface crack

The presence of compressive thermal residual stresses provides the interface with additional protection against the initiation of damage, as has been explained in the previous section. In any case, once the failure is initiated it is also necessary to analyse the influence of thermal residual stresses over the growth of the first debonds. To this end the model appearing in Fig. 2a is used in this section to carry out, by means of the BEM, an analysis of the interface crack growth under the combined action of an external tensile load ($\sigma_0 = Y_T$) and a thermal decrease of 80ºC.

The results obtained, in terms of G versus the debonding angle θ_d, are presented in Fig. 3 for the case under study (named as $\Delta T = \text{-}80^{\circ}C$ in the Figure), which considers both thermal residual stresses and those derived from the load σ_0, and for the case of single action of σ_0 ($\Delta T = 0^{\circ}C$ in the Figure), used as a reference in this analysis and a basis for the conclusions presented in [3].

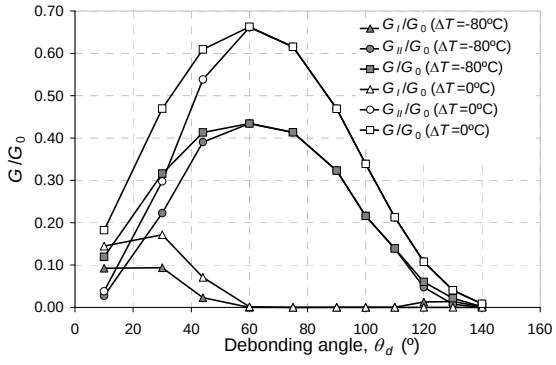

Figure 3. G evolution versus θ_d ($\Delta T = 0^{\circ}C$ and $\Delta T = -80^{\circ}C$ cases).

The evolutions observed for both cases are similar, not only for the global value G but also for the modes partition, though lower values in all evolutions are obtained for the $\Delta T = \text{-}80^{\circ}C$ case. This result makes it possible to also predict a protective effect of the thermal residual stresses on the interface against the propagation of the interface crack, coinciding with the protective action against the initiation of failure already deduced in the

previous section. In spite of the apparent similarity of the evolutions associated to $\Delta T = 0^{\circ}C$ and $\Delta T = \text{-}80^{\circ}C$, the more relevant presence of Mode II for $\theta_d < 60^{\circ}$ stands out for the $\Delta T = \text{-}80^{\circ}C$ case in comparison with the $\Delta T = 0^{\circ}C$ case, which evidences an earlier development of the finite contact zone at the interface crack. In this sense, the appearance of the contact zone for the $\Delta T = \text{-}80^{\circ}C$ case specifically takes place for $\theta_d = 50^{\circ}$, a lower value in comparison with the $\Delta T = 0^{\circ}C$ case ($\theta_d = 60^{\circ}$). Coherently, the length of the contact zone is larger in the $\Delta T = \text{-}80^{\circ}C$ case than in the $\Delta T = 0^{\circ}C$ case, for all θ_d considered.

In order to perform predictions about the interface crack growth it is necessary to have an estimation of the critical value of G, G_c, which depends on the evolution of the fracture mode mixity, defined by the local phase angle, ψ_K, and therefore a function of θ_d. The law considered in this work for G_c is based on the simplified empirical proposal by Hutchinson and Suo [4]:

$$G_c(\psi_K) = G_{1c}\left(1 + \tan^2(1-\lambda)\psi_K\right) \tag{2}$$

where G_{1c} is the critical value of G_c for Mode I and λ is the fracture mode sensitivity parameter. ψ_K has been calculated following:

$$\psi_K = 0.5 \arccos\left[F(\varepsilon)^{-1} \frac{G_I - G_{II}}{G_I + G_{II}} \right] \tag{3}$$

where $F(\varepsilon) = 1 + \left(\pi^2/3 - 2\right)\varepsilon^2 + O(\varepsilon^4)$, ε being the oscillatory index which, for the bi-material system employed, takes the value $\varepsilon = -0.074$.

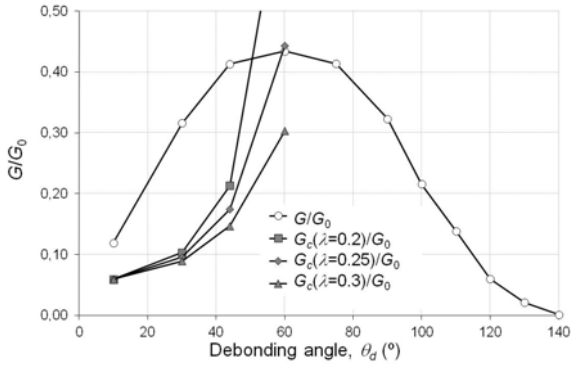

Figure 4. G and G_c for the interface crack ($\Delta T = -80^{\circ}C$).

This approach was already employed in [3] to predict the growth of the interface crack for the $\Delta T = 0^{\circ}C$ case, making use of three different values of λ (within the range of typical values): $\lambda = 0.2, 0.25, 0.3$. In that case, due to the absence of direct experimental data, the value of G_{1c} chosen for each λ was forced to fulfill the expression $G = G_c(\psi_K)$ for $\theta_d = 5^{\circ}$ (where $G(\theta_d = 5^{\circ})$ has been obtained by interpolation). The results provided by the

comparison between the values of G and G_c calculated in this way predicted an unstable growth of the interface crack up to θ_d in the range 60º-70º.

The same process has been implemented in the present work for the case including the thermal residual stresses, $\Delta T = \text{-}80^{\circ}C$. The results obtained for the comparison between G and G_c are shown in Fig. 4 (G_{1c} being chosen following the same criterion previously employed for the $\Delta T = 0^{\circ}C$ case). The results shown in Fig. 4 predict an unstable growth of the interface crack up to θ_d in the range 50º-70º, a similar conclusion to that already deduced for the $\Delta T = 0^{\circ}C$ case, though this range is wider at its lower bound. Thus, this range of termination of the unstable growth and of change in the propagation mode seems to be a favourable place for the development of a new stage of the mechanism of damage, i.e. the kinking of the interface crack towards the matrix and its propagation through it.

2.4 Kinking

The prediction of the interface crack kinking towards the matrix, once the period of unstable growth at the interface has finished, consists of two steps: the search for the preferential direction of the incipient crack in the matrix and the evaluation of the possibility of this change in the propagation of the crack.

Referring to the first aspect, the application of a kinking criterion, for instance Maximum Circumferential Stress criterion (MCS criterion):

$$\sigma_{\theta\theta}(r,\theta_{kink}) = \max_{\theta} \sigma_{\theta\theta}(r,\theta) \tag{4}$$

in the neighbourhood of the interface crack tip within the θ_d range of termination of unstable growth, allows the most favourable direction of the incipient crack in the matrix to be predicted [3] . The application of this criterion for the $\Delta T = 0^{\circ}C$ case concluded that if kinking took place it would occur for $\theta_d = 60^{\circ}\text{–}70^{\circ}$ in a direction approximately normal to σ_0 [3].

The same analysis is presented here for the $\Delta T = \text{-}80^{\circ}C$ case, studying the circumferential stress state in the neighbourhood of the interface crack tip at the positions $\theta_d = 60^{\circ}$ and $\theta_d = 70^{\circ}$ and for points located on two circumferences (radii $r = 0.001a$ and $r = 0.01a$) centred at the tip. The numerical results are shown in Fig. 5, proving that, in accordance with the reference of the angle θ considered in the Figure, the maximum circumferential stress is produced approximately in the same direction as in the $\Delta T = 0^{\circ}C$ case.

With reference to the possibility of kinking taking place for the $\Delta T = \text{-}80^{\circ}C$ case, the energy release rate of the incipient crack in the matrix, G^m, has been calculated using the model presented in Fig. 2b and assuming the direction of the incipient crack to be perpendicular to the external load σ_0, in a similar way to the study previously performed in [3] for the $\Delta T = 0^{\circ}C$ case. This study has been carried out for different positions of the interface crack.

The length of the crack in the matrix considered has been 0.013a (the minimum value permitted by the discretization employed).

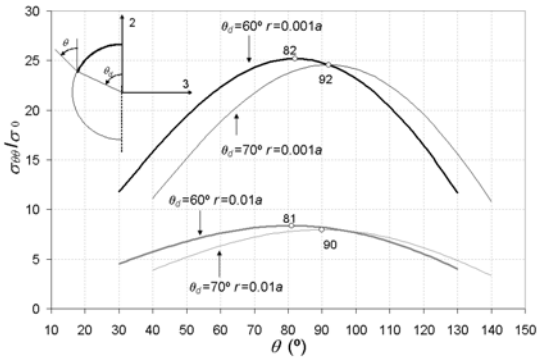

Figure 5. $\sigma_{\theta\theta}$ distribution around interface crack tip ($\Delta T = -80^{\circ}C$ case).

The results corresponding to the $\Delta T = -80^{\circ}C$ case are presented in Fig. 6 jointly with the evolution of G for the interface crack (named as G^{int} in the graph), the higher level reached by G^m in comparison with G^{int} standing out here. It is also necessary to point out that the obtained G^m values correspond to Mode I, whereas G^{int} is due to Mode II. The relative position of both distributions ($G^m(\theta_d)$ and $G^{int}(\theta_d)$) and the fact that in the range of termination of unstable growth of the interface crack the character of G^{int} turns into Mode II, whereas that associated to G^m corresponds to Mode I and shows unstable behaviour, favours, from an energetic point of view and in comparative terms, the possibility of crack kinking towards the matrix. Finally, taking into account that G_{Ic}^m and G_{IIc}^{int} in the references consulted provide, in the zone of recommended values, a range of values that fulfills $G_{IIc}^{int} > G_{Ic}^m$, the possibility of kinking towards the matrix is found to be the most plausible option. This conclusion agrees with that previously obtained in [3] for the $\Delta T = 0^{\circ}C$ case.

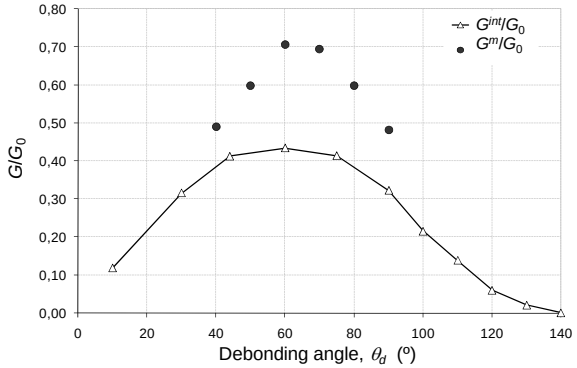

Figure. 6. Comparison between G^m and G^{int} ($\Delta T = -80^{\circ}C$ case).

3. Experimental results

Tension tests were planned on 90º unidirectional specimens in order to check the conclusions derived from the numerical study presented in the previous section. To fulfill this objective it was necessary to cure the same material at different temperatures (thus promoting a different value of thermal residual stresses) and check whether the strength of the material was affected.

After careful and intense testing, two different curing cycles, based on [5], were selected for the manufacturing of twelve-ply unidirectional graphite-epoxy laminates:

A) Cycle 1: Heat to 121ºC in 30', hold at 121ºC for 1h, heat to 177ºC in 30', hold at 177ºC for 3h and cool to room temperature.
B) Cycle 2. Heat to 121ºC in 30', hold at 121ºC for 48h and cool to room temperature.

For the cases under consideration glass transition temperatures were 149 ºC for the laminate cured at 121ºC and 156 ºC for the laminate cured at 177ºC, indicating a similar curing level in both cases.

With reference to the strength results found in the tension tests a mean value of 38.4 MPa was obtained for the specimens cured at 121ºC whereas 48.6 MPa was the mean strength for the specimen cured at 177ºC. Thus, a 27% increase in strength is found for the specimens cured at 177ºC with reference to the specimens cured at 121ºC. This experimental result leads to the conclusion that the presence of higher thermal residual stresses has a protective effect in transverse tension tests for unidirectional laminates, which is in agreement with the conclusions previously obtained from the numerical analysis.

4. Conclusions

The numerical results obtained from the present single fibre models clarify, at least for the case of dilute fibre packing, the effect of thermal residual stresses in the development of the inter-fibre failure under tension at micromechanical level, concluding that they have a protective effect against inter-fibre failure generation, though the phases of the mechanism of damage seem not to be significantly influenced by their presence. The experimental results obtained from transverse tension tests, carried out on unidirectional laminates, are in agreement with the numerical results.

Acknowledgements

The work was supported by the Spanish Ministry of Education and Science (Project No. MAT2009-14022) and Junta de Andalucía and European Social Fund (Projects No. TEP-04051 and TEP-04071). The authors thank Dr. E. Graciani whose BEM code has been used.

References

[1] París F. *A study of failure criteria of fibrous composite materials*. NASA/CR-2001-210661, 2001.
[2] París F., Correa E., Cañas J. Micromechanical view of failure of the matrix in fibrous composite materials. *Compos Sci Technol*, 63, pp 1041-1052 (2003).
[3] París F., Correa E., Mantič V. Kinking of transverse interface cracks between fibre and matrix. *J App Mech*, 74, 4, pp. 703-716 (2007).
[4] Hutchinson J.W., Suo Z. Mixed mode cracking in layered materials. *Adv App Mech*, 29, pp. 63-191 (1992).
[5] Crasto A.S., Kim R.Y. On the determination of residual stresses in fibre reinforced thermoset composites. *J Reinf Plast Comp*, 12, pp. 545-558 (1993).